ANALYSIS OF THE INTERACTION OF NEIGHBOURING LAMINAE IN FIBRE-REINFORCED PLASTICS DURING CYCLIC LOADING

T. Hensel
Technische Universität Darmstadt
Fachbereich 16 – Maschinenbau, Konstruktiver Leichtbau und Bauweisen
Petersenstraße 30, 64287 Darmstadt, Germany

OVERVIEW

A layer-wise strength analysis of laminates, based on an actionplane-related strength criterion leads to realistic results not only with quasistatic loading but also with cyclic loading. When inter-fibre fracture (IFF) cracks occur in laminae e.g. during cyclic loading the laminate stiffness is reduced and is determined by degradation models. The local increase in stress in the undamaged laminae, adjacent to the laminae affected by an IFF, is not being accounted for. Hence, this notch effect - caused by IFF - leads to a much earlier failure of the lamina as predicted in current failure criteria. In order to determine the influence of notch effects and the resulting reduction factors of two adjacent laminae, FEM analyses and tests were performed. The analysis shows a significant decrease in fatigue strength of up to 50% compared to a Classical Laminate Theory (CLT) predicted undisturbed UD lamina.

1. INTRODUCTION

A lot of different investigations on the behaviour of laminates under cyclic loading were done in the past and also different theories were adopted to. Still, there is a need for better prediction of the fatigue behaviour of laminates until its failure through fibre fracture.

One of the most precise methods for layer-wise strength analyses is *Puck*'s criterion. It's a physically based criterion and relates to actionplanes in laminates. Since the criterion works layer-wise the influence of adjacent laminae is neglected. Hence, the damage in adjacent laminae is not considered as well. Nevertheless, if 2 laminae are separated via a fracture stopping lamina, the results gained for cyclic loading so far are very promising [1]. In order to overcome this the laminate must be seen as it is mostly found in parts. By doing this fracture stopping laminae are not considered and adjacent laminae can interact freely with each other. In this case, there is no exact prediction of the laminate life available. From a designing engineer's point of view life prediction causes additional cost since long-winded and pricy cyclic tests need to be performed. Furthermore unknown effects like the effect of IFF on an undamaged lamina as described above are often compensated by exaggerated factors of safety.

Further reasons for no excessive use of fracture stopping lamina are in economical and technical nature. Firstly, this will lead to higher manufacturing cost and secondly, lightweight design is not in strong consideration anymore. Hence, selective use of fracture stopping lamina should be made there where minor damages lead to rapid failure of the whole part.

2. FEM ANALYSES

There are two different models investigated, a 2D-model (not shown in this paper) and a 3D-model. The models were generated and simulated with *ANSYS*®, *Release 8.1*. All used length an width parameters are dimensionless. The results e.g. stresses are given in common units. The models are subject to a given displacement in such a way that the 0°-fibre faces 100N/mm² (=100MPa).

2.1. The 3D-FEM-Model

2.1.1. Geometry and adjustable parameters

In FIG 1 the micro-mechanical 3D-FEM-model with its dimensions is shown (in this case with a 70° transverse

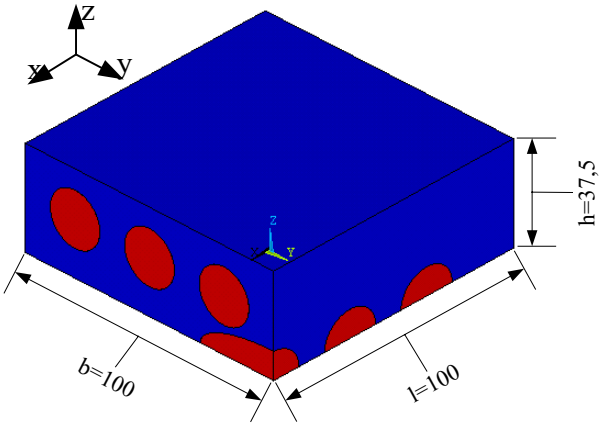

FIG 1. 3D-FEM-model with dimensions, shown with a 70° angle in the transverse lamina. Fibres are shown in red, matrix in blue.

oriented lamina). The red areas are the fibres and the blue areas are the matrix. The model is using the x-y-plane as a symmetry plane and hence saving simulation time. The model consists of 2 laminae. While the upper lamina is oriented in the direction of load (0°-lamina), the lower lamina can be adjusted in its angle from 0°-90° to the upper lamina. The lower lamina will be further called the transverse lamina. The fibre diameter in this study equals 20 and the distance between the transverse fibres and the 0°-fibres (the distance between upper und transverse lamina, respectively), *af*, is varied during the study. Furthermore the angle between the laminae and the length

of the crack are varied.

2.1.2. Generation of IFF in 3D-FEM-Model

In FIG 2 the length of the crack, *a*, is shown. It is situated at the middle fibre of the transverse lamina and has got a semi-cylindrical shape. With this initial crack the local stress increase in the upper middle 0°-fibre due to this crack is investigated.

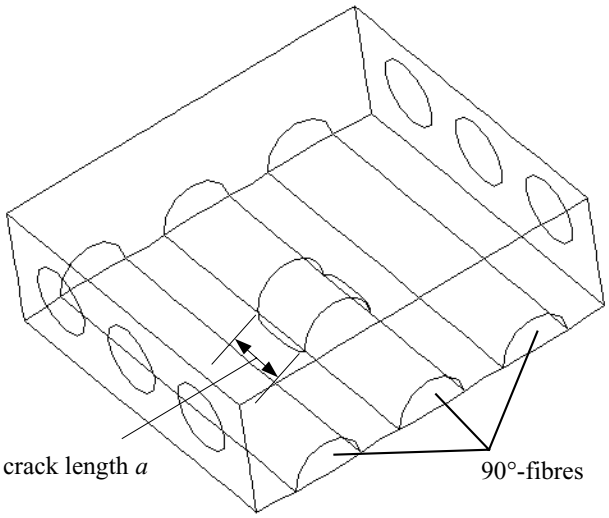

FIG 2. Wire frame model to show the IFF crack with the length *a*.

For better understanding the opening crack (70 times exaggerated) is shown in FIG 3.

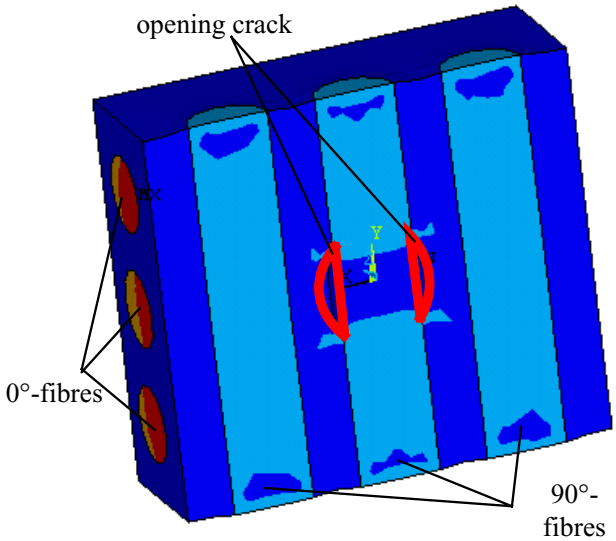

FIG 3. Opening crack at the middle of the transverse fibres (70 times exaggerated) due to a displacement in x-direction

2.1.3. Boundary conditions

In FIG 4 the boundary conditions of the 3D-FEM-model are shown. The model is subjected to a displacement in x-direction (direction of 0°-fibres) at its boundaries. The displacement is shown in light blue. The displacement is calculated in such a way that a (tensional) stress of 100N/mm² results in the 0°-fibres. Furthermore the model is constrained in y- and z-direction.

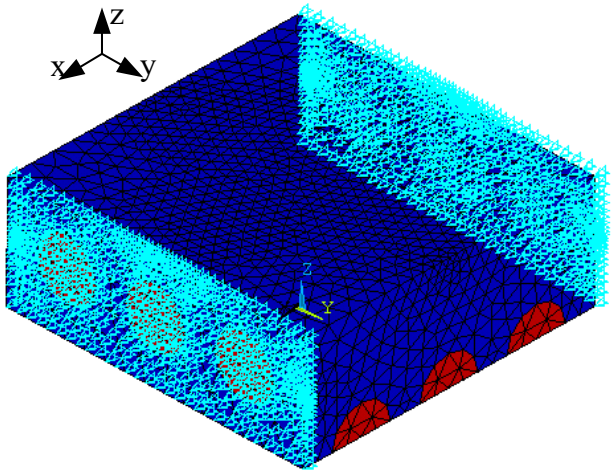

FIG 4. Boundary Condition of the 3D-FEM-model

2.1.4. Path to Identify the Stress Distribution

In FIG 5 the path is shown which is used to retrieve the resulting stresses. The path is shown in blue. It runs along above the transverse oriented fibres (here: with a part of the middle transverse fibre affected by IFF), in the middle 0°-fibre. The stresses in this fibre are influenced by the narrow situated IFF.

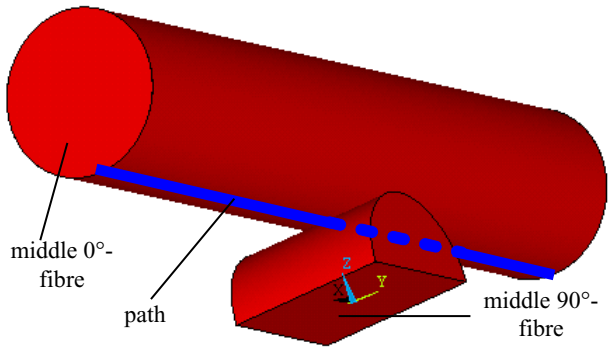

FIG 5. Path to identify the stresses in the middle 0°-fibre

2.1.5. Results and Discussion 3D-Model

In this chapter 3 parameters are investigated and analysed. These are the angle of the transverse oriented lamina, the distance of the laminae and the length of the crack at the middle transverse fibre. All parameters have a different impact on the local stress increase in the 0°-fibre.

In FIG 6 the middle 0°-fibre is shown. The resulting v. Mises stresses can be distinguished by the scale. In the red area the maximum stress in the 0°-fibre can be found. It amounts to 111N/mm². This area is situated directly above the not shown crack which is located at the middle transverse fibre (in this case 90° angle). The local stress increase is fading away in a radial manner and has got roughly the size of a diameter of a fibre. The greenish area

shows places where the local area has faded away completely. The bluish area is about 10N/mm² below the adjusted value of 100N/mm². In this area the 0°-fibre is crossed by the outer transverse fibres. This leads possibly to effects of transverse contraction followed by a bending of the 0°-fibre and hence, to an overlay of compressive stress.

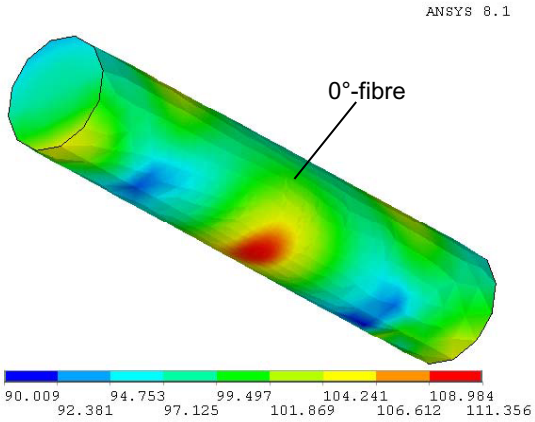

FIG 6. Distribution of von Mises stress in the 0°-fibre

2.1.5.1. Variation of Laminae Angle

In FIG 7 the local maximum stress increase of the 0°-fibre at different angles is shown. The stresses are related to the adjusted stress of 100N/mm² in the 0°-fibre. The parameter for the distance of the laminae, *af*, is held constantly at 0.2 and the crack length *a* at 20, respectively.

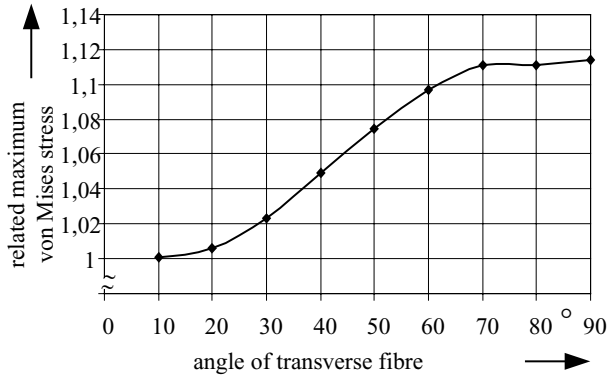

FIG 7. Related maximum von Mises stress of the 0°-fibre over the angle of the transverse fibres. Lamina distance *af* constant 0.2 and crack length *a* constant 20

The local increase of stresses reaches their maximum with a 90° transverse lamina, as expected. The local increase in stress accounts for 12%. The values for the angles 70°, 80° and 90° are almost alike which leads to the conclusion that the IFF has got the same notching effect for these three angles. For very small angles of the transverse lamina (10°) the increase of stress is not existent anymore.

2.1.5.2. Variation of Laminae Distance

In FIG 8 the influence of the distance of the laminae, *af*, on the local increase of stress is shown. The distance is varied from 0.1 to 0.4 while the transverse lamina angle is constantly 90° and the length of the crack a is kept constant at 20. In FIG 15 it can be clearly seen that the larger the distance between the laminae gets the lower the local increase in stress in the 0°-fibre gets. At big

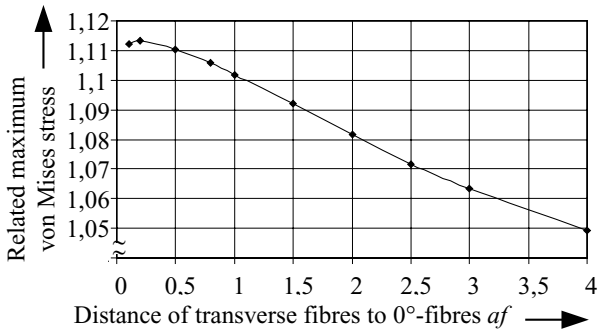

FIG 8. Related maximum von Mises stress of the 0°-fibre over the distance of laminae *af*. Transverse angle constant 90° and crack length *a* constant 20.

distances, that are approximately bigger than half the fibre's diameter the crack has no more influence on the stress increase in the 0°-fibre. The maximum stress increase in the 0°-fibre accounts for 11%.

2.1.5.3. Variation of Crack Length

In FIG 9 the influence of varying the length of the crack at the middle transverse fibre, *a*, is shown. In this case the

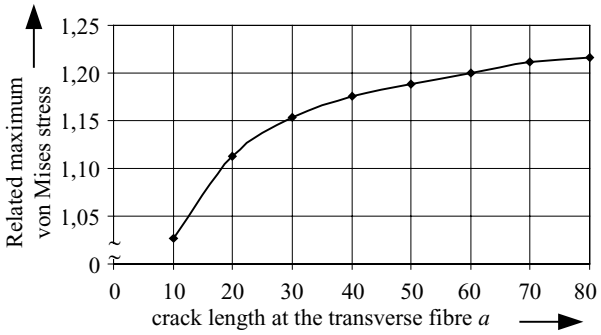

FIG 9. Related maximum von Mises stress in the 0°-fibre over the crack length *a*. Transverse angle constant 90° and laminae distance constant 0.2.

distance *af* is kept constant at 0.2 and the transverse lamina angle at 90°, respectively. FIG 9 shows the related maximum v. Mises stress in the 0°-fibre over the crack length. First, the local increase in stress in the 0°-fibre increases fast with growing crack length at the transverse fibre. Later the slope becomes more and more declining but convergence can not be seen. A further increase of the crack length is limited due to the dimensions of the model (total width of $b = 100$) and also due to the growing

influence of the boundary. In total the maximum increase accounts for 22% at a crack length of *a* = 80.

2.2. Resume of FEM-Models

The 3 investigated parameters , transverse lamina angle, distance of laminae *af* and crack length *a* have got an influence on the stress increase of the 0°-fibre. The results for the 2D- (not shown) and the 3D-model show a good correlation. The crack length at the transverse fibre has got the biggest influence on the stress increase in the 0°-fibre. The maximum stress increase accounts for 22%. The shown case that the crack length reaches its maximum can be found in reality as well. The IFF extends to the whole width of the laminate. Thus, an increase in stress of at least 22% can be expected in reality.

3. EXPERIMENTAL STUDIES

3.1. Specimen's Geometry

In FIG 10 the specimen for the chosen 3-point-bending fatigue tests and its dimensions are shown. The dimensions are chosen in order to fit the given test stand (FIG 20) in length and width. The specimen is not clamped and thus early failure due to IFF or fibre fracture close to the clamping can be avoided.

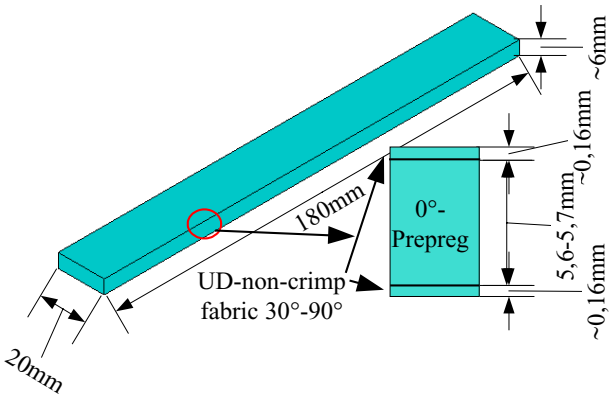

FIG 10. Display of the standard specimen with its laminae set-up

In order to investigate the influence of IFF on adjacent laminae and fibres, respectively, a special layout of the specimen is necessary. To capture the notch effect the specimen was divided in 3 parts. For the 0°-laminae prepreg is used. The upper and lower lamina consists of uni-directional non-crimp fabrics which is draped on the 0°-prepreg in angles varying from 30°-90°. This method is used to show the influence of the angle on the 0°-fibres. Considering that IFF occurs already during the first deflection of the specimen those IFF cracks have a notching effect on the adjacent 0°-fibres.

3.2. Material

In TAB 1 the used materials for the prepreg are listed. Furthermore for the draping of the specimen a unidirectional non-crimp fabric *Type UD EST 250* (unidirectional non-crimp fabric with PES-fixation grid) of *Haufler Industrievertretungen* is used. The uni-directional non-crimp fabric has got an area weight of $m_{fabric} = 250\,g/m^2$. The fibres have a density of $\rho = 2{,}54\,g/cm^3$.

IFC-Prepreg, *IFC Composite GmbH*; Name *UD-GL SE1500*			
Matrix		Fibre	
Name	*Bakelite EPR 05322+EPH 778+EPC120*	Name	*OC SE 1500 2400*
Manufacturer	*Bakelite AG*	Manufacturer	*OWENS CORNING*
Young's modulus	3450 ± 250 N/mm²	Type	E-Glas
T_G	115°C	Tex-number	2400g/km
	Harz	fibre diameter	17µm
Name	*Bakelite EPR 05322*	Young's modulus	83000 N/mm²
Type	Epoxidharz	number Rovings/width	24
weight	100		
	Härter	Number layers	13
Name	*Bakelite EPH 778*		
weight	15		
	Beschleuniger		
Name	*Bakelite EPC 120*		
weight	5		

TAB 1. Material data for prepreg of *IFC Composite GmbH* [2],[3]

3.3. Manufacturing of Specimen

In FIG 11 the principle of manufacturing the specimen can be seen. The unidirectional non-crimp fabric is positioned in a certain angle (here: 30°). Afterwards the unidirectional prepreg is positioned in 0°-direction.

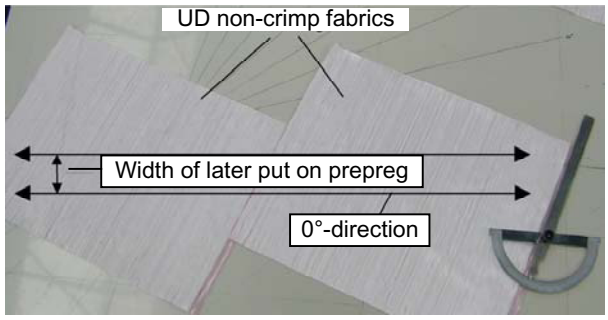

FIG 11. Adjustment of angle for the UD non-crimp fabric during draping of the prepreg specimen (here: 70° angle)

The draped prepreg is positioned in a compression mold, heated up and hardening under defined pressure. The finished prepreg plate is taken out of the compression mold and after cooling down it is annealed for 3 hours at 160°C. After annealing the plate is sawn into the desired specimen size with a diamante saw in order to damage the fibres as little as possible. Concluding, the edges of the specimen are deburred and a small chamfer is applied.

3.4. Preliminary Static Tests and Microscopy

In FIG 12 the test stand for 3-point-bending is shown. The test frame is mounted on a hydraulic cylinder which is moving the punch via a piston rod and enables the load transmission into the specimen.

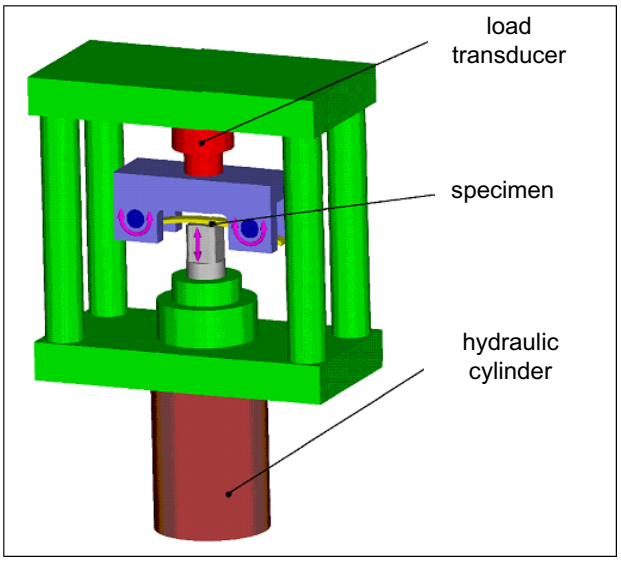

FIG 12. Set-up of 3-point-bending test stand [4]

In order to document damage progress a 90°-0°-90°-specimen (FIG 10) was investigated via microscope after gradual load increase. A certain area was assigned in order to investigate the same area after each load step. In

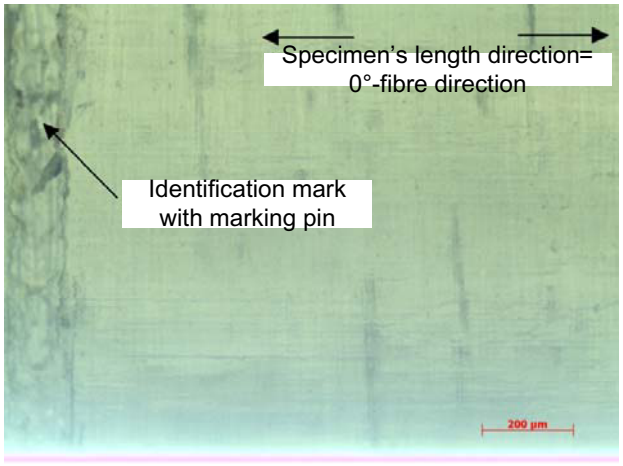

FIG 13. Top view on unloaded specimen at 50 times magnification

FIG 13 the unloaded specimen is shown from top view and in FIG 14 from side view, respectively. For better understanding the border of the 0°/90° lamina is marked. It can also be seen that there is no theoretical configuration of the fibres (quadratic or hexagonal configuration) but rather a random distribution with areas of high matrix content and other area with high fibre packing.

In FIG 15 the specimen is shown with 500 times magnification. It can be clearly seen that the transverse fibres are very close to or even touch the 0°-fibres. Considering an IFF evolving at the transverse fibres, this would result in a direct influence on the 0°-fibres as assumed in the FEM-model.

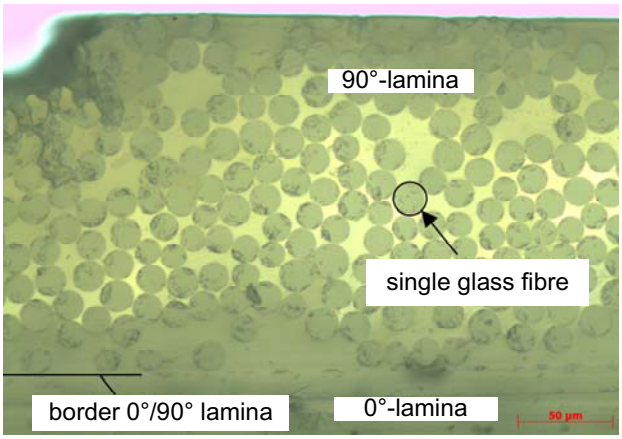

FIG 14. Side view on unloaded specimen at 200 times magnification

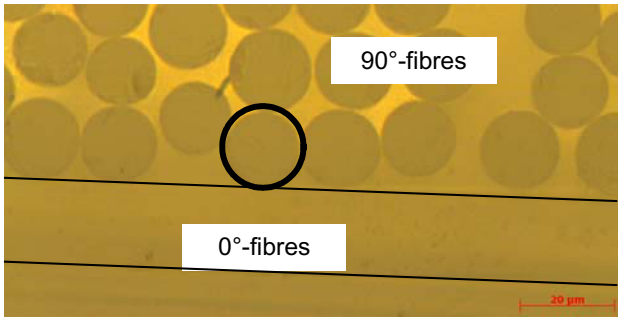

FIG 15. Side view on unloaded specimen at 500 times magnification. Proximity of transverse fibres to 0°-fibres

When loading the specimen first failures can be seen. First, only IFF cracks are occurring, as can be seen in FIG 16.

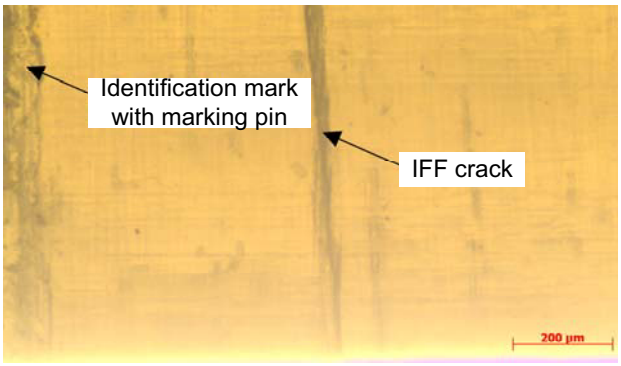

FIG 16. Resulting IFF after first loading (top view)

The IFF crack is almost spread over the whole width of the specimen. Over the length of the specimen a couple IFF cracks can be seen (not shown in FIG 16). In FIG 17 a typical IFF crack is shown in side view. The crack develops from the interface failure of fibre and matrix. The crack covers half of a single fibre and "jumps" to the proximate fibre. The crack initiates at the upper boundary (edge) of the specimen and spreads in a s-shaped way until it reaches the 0°-lamina.

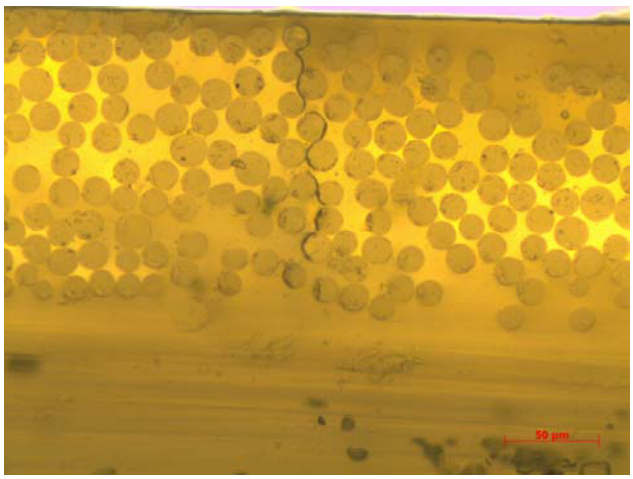

FIG 17. Progress of an IFF crack in a 90°-lamina (200 times magnification)

After increasing the load the specimen shows a characteristic damage state (FIG 18), i.e., that a saturation of IFF cracks can be determined (lengthwise).

FIG 18. Multiple IFF cracks after higher loading (top view, 50 times magnification)

In FIG 19 the direct influence of an IFF crack on fibre

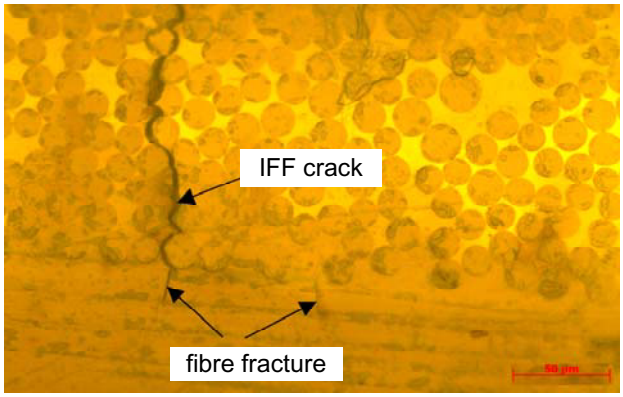

FIG 19. Fibre fracture in direct proximity of an IFF crack (200 times magnified)

fracture can be seen. After running through the complete lamina the IFF crack notches the adjacent 0°-fibre in a way that it cracks. Furthermore FIG 19 shows one more fibre fracture which occurs in some distance of the first fibre fracture. This distance is not defined but rather random. Nevertheless, stresses, after being zero in the area of the left fibre fracture directly below the IFF crack, rise to an extent that the same fibre breaks again (right fibre fracture) at a distance of 50µm.

3.5. Bending Fatigue Tests

All manufactured specimen are tested in a 3-point-bending fatigue test. The tests are displacement controlled and a defined strain ratio of $R = \varepsilon_{lower} / \varepsilon_{upper} = 0.1$ is applied. Furthermore all bending fatigue tests are performed as a single level test, i.e., the displacement time function is sinusoidal and has a constant amplitude. The test frequency is $f = 10$ Hz at all tests. For a stop criterion a loss of 5% of the specimen's dynamic stiffness is considered.

3.5.1. Damage Progress in a 90°-0°-90° Specimen

In this and the following chapter the damage progress is being followed by consecutive imaging of a 90°-0°-90° and an exclusively 0°-specimen after several cycles.

In FIG 20 the middle area (lengthwise) of a 90°-0°-90° specimen (upper strain of 0°-lamina: 1.14 %) after 40 000 cycles and a stiffness loss of 0.82 % is shown (top view). The specimen shows a saturation of IFF cracks (thin white lines) which run over the whole width of the specimen (from edge to edge). The IFF cracks show a characteristic damage state, i.e., an almost constant distance of ca. 200µm. Furthermore an onset of delamination can be seen at the upper edge of the specimen. The thicker white lines are not considered. They are polyether sulfone (PES) fixation grids for the fibres of the non-crimp fabrics.

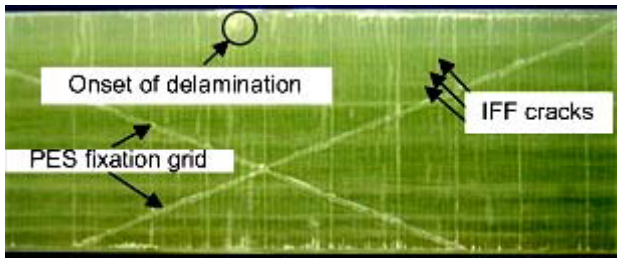

FIG 20. 90°-0°-90°-specimen after 40 000 cycles and stiffness loss of 0.82 %

Further progress can be seen after 100 000 cycles in FIG 21. Many local delaminations occur in the middle of the specimen (widthwise) while the outer delaminations spread at the edges of the specimen not only lengthwise but also to the middle of the specimen (widthwise).

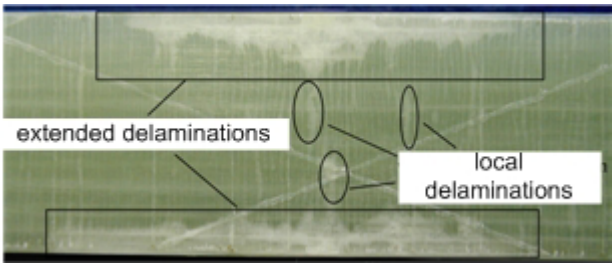

FIG 21. 90°-0°-90°-specimen after 100 000 cycles and a stiffness loss of 2.05 %

After 200 000 cycles (FIG 22) the area of the middle delaminations expands and connects the delaminations at the edges of the specimen. The specimen is almost facing the 5 % stiffness loss. The picture of damage for that case is not different to that at 200 000 cycles. Thus it is not shown in this paper.

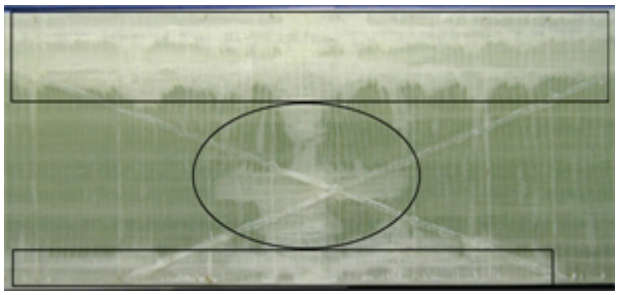

FIG 22. 90°-0°-90°-specimen after 200 000 cycles and a stiffness loss of 4.1 %

3.5.2. Damage Progress in an exlusive UD-Specimen

In FIG 23 the damage state after 60 000 cycles of an exclusive 0°-specimen at an upper strain of 1.9% can be

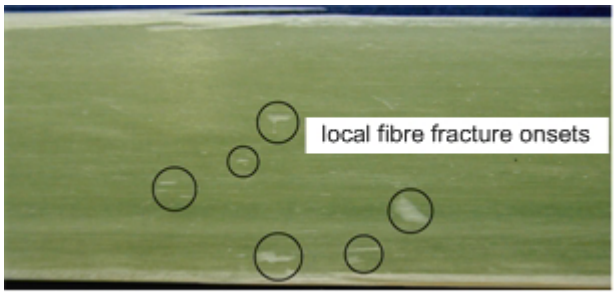

FIG 23. 0°-specimen after 60 000 cycles and a stiffness loss of 1.34 %

seen. The fibre fractures are situated mainly at the edge of the specimen but also in the middle. The single fibre fractures directly build clusters of fibre fracture which makes the fractures visible as plane damages.

In FIG 24 the damage progress after 100 000 cycles can be observed. The single fibre fractures build clusters of fibre fracture and join each other. Furthermore those fibre fracture clusters build delaminations over larger areas and reduce the stiffness of the specimen measurably.

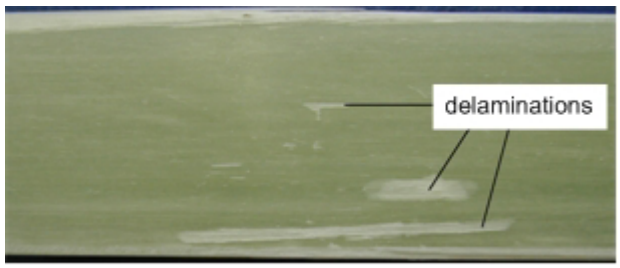

FIG 24. 0°-specimen after 100 000 cycles and a stiffness loss of 2.24 %

In FIG 25 the specimen is shown after failure (stiffness loss of 5 %). The delaminations shown in FIG 24 were growing to a big extent and are now connected to each other. They build big areas of splintering. These areas account for half of the width of the specimen and don't transfer any load anymore.

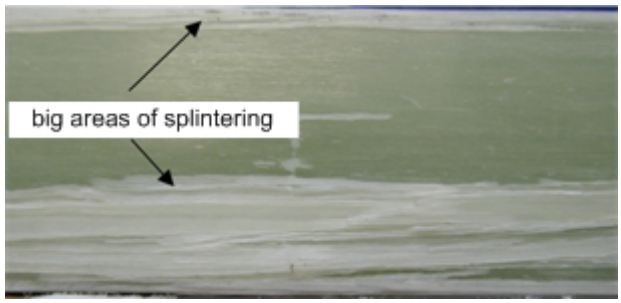

FIG 25. 0°-specimen after 222 000 cycles and a stiffness loss of 5 % (failure)

3.6. Results and Discussion

3.6.1. Woehler Curves of Investigated Specimen

In this chapter three different specimen – all tested in bending fatigue tests - are compared to each other. These are the exclusive 0°-specimen (UD-specimen), a specimen with a 90°-0°-90° set-up and a 30°-0°-30° set-up (FIG 10), respectively.

In FIG 26 the single logarithmic Woehler curves for the 3 specimen types are shown. The Woehler curves are deduced from the regression lines of the single investigation points (upper strain values). The regression lines are retrieved by the Least Squares Method. The upper strain, shown at the ordinate of the diagram, is calculated at the upper edge for the exclusive 0°-specimen and at the border of the 0°/90°- and 0°/30°-lamina for the 90°-0°-90°-/30°-0°-30°-specimen, respectively. By doing this, comparability between the different set-ups is given, since the 90°-0°-90°- and the 30°-0°-30°-specimen are thicker than the exclusive 0°-specimen and hence no fair comparison is possible. Furthermore failure of the 0°-lamina is of major interest. Thus, the strain at the edge of the 0°-lamina should be the same for all investigated specimen.

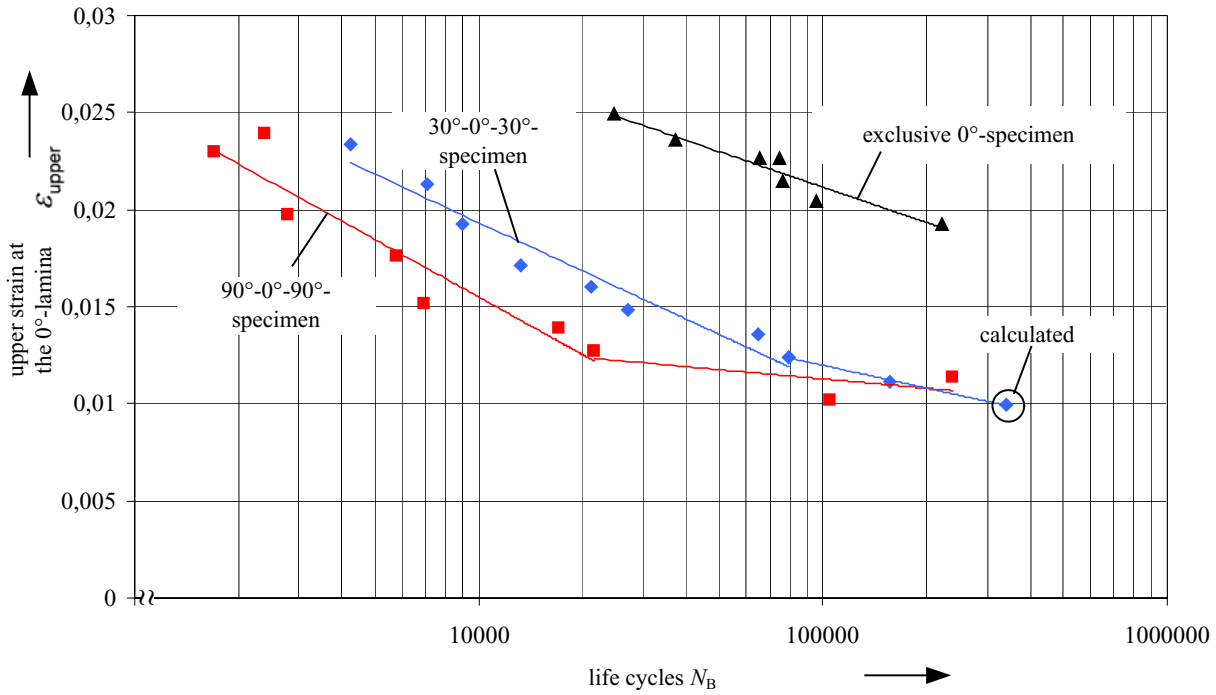

FIG 26. Woehler curves (single logarithmic) of exclusive 0°-specimen, 90°-0°-90°-specimen and 30°-0°-30°-specimen (R = 0.1, f = 10Hz). Stop criterion is a loss of 5% of the specimen's dynamic stiffness. The "calculated" specimen was not run until this 5% loss but was extrapolated out of the stiffness cycle diagram.

In FIG 26 the influence of the 90°-and 30°-lamina(e), respectively, on the failure's point of time can clearly be seen. The 90°-0°-90°-/30°-0°-30°-specimen, where the 0°-lamina(e) is influenced by the transverse lamina(e), show much earlier failure than the exclusive 0°-specimen. The Woehler curves are not parallel to each other. While the slope for the 90°-0°-90°-specimen is bigger than for the exclusive 0°-specimen, the slope difference for the 30°-0°-30°-specimen is not that big.

For the 90°-0°-90°-specimen the Woehler curve shows a kink or a strong bending. Present investigations assume that FRP doesn't show a kink in comparison to steel [5]. The main reason for this is the fact, that with FRP the number of cycles cannot reach "endurance strength" (at least for a test frequency $f = 10$ Hz) since the number of cycles would be far too big. The damages in the 0°-lamina – induced by the 90°-lamina in the case for the 90°-0°-90°-specimen – are to such an extent that a kink in the Woehler curve can be seen at relatively low cycles. This kink or strong bending of the Woehler curve is a new aspect for FRP which must be further investigated. For even lower loading (smaller values for the upper strain in the 0°-lamina) the transition to endurance strength can be expected.

Looking at the number of cycles for the exclusive 0°-specimen and the other specimen type a factor of 20 to 30 lies between them. If a 90°-0°-90°-specimen fails at 3000 cycles, an exclusive 0°-specimen fails at 90 000 cycles for the same strain level. For the 30°-0°-30°-specimen the factor is a bit smaller, i.e., that a smaller angle (related to the 0°-direction) has less impact on the failure of the whole specimen. The IFF cracks of a 30°-lamina don't have notching influence as big as the IFF cracks in a 90°-lamina, but still factor 20 (means 20 times earlier failure than an exclusive 0°-specimen at the same strain level).

In FIG 27 another approach is shown. The stresses parallel to the 0°-fibres are compared at the same number of cycles. It can be clearly seen that there is a difference in stress between the 0°-specimen and the

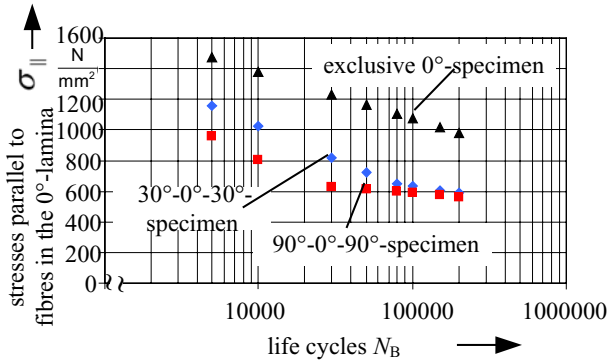

FIG 27. Stresses parallel to fibres over life cycles

other specimen types. Thus, the 30°-0°-30°-/90°-0°-90°-specimen – notched by IFF cracks - are additionally loaded by that difference. For life cycle numbers of $N_B = 5 \cdot 10^3$ to $N_B = 5 \cdot 10^4$ the stress difference to the 0°-specimen accounts for $500 - 600 N/mm^2$ for the 90°-0°-

90°-specimen and $300-400\,\mathrm{N/mm^2}$ for the 30°-0°-30°-specimen, respectively. This corresponds to a strength reduction of 35-50 % for the 90°-0°-90°-specimen and 20-40 % for the 30°-0°-30°-specimen, respectively, depending on the focused stress level. When the curves start bending at higher cycles (50 000 cycles and 80 000 cycles respectively) the stress increase becomes smaller.

3.6.2. Modified Woehler Curves

In the previous chapter it was shown that IFF cracks have a severe influence on the failure of the laminate. Nevertheless, big areas of delaminations in the transverse lamina (90°- and 30°-lamina, respectively) were observed. Hence, this lamina (90°- and 30°-lamina, respectively) doesn't take any load or a very reduced load and the specimen's stiffness of bending is lower than at the beginning. Thus, a worst case is considered where a specimen's upper lamina (90°- and 30°-lamina, respectively) is completely peeled off, i.e., that the lamina's Young's modulus is set to zero and the specimen has got a lower stiffness from the beginning. That must be considered by the stop criterion and thus, the loss of stiffness is related to the lower stiffness of the specimen. This leads to stiffness losses of 7.5% for the 90°-0°-90°-specimen and 10.5% for the 30°-0°-30°-specimen, respectively, which are taken as stop criteria. The increased stop criteria lead to higher cycles (FIG 28). In order to retrieve the new life cycles the test with the specimen were continued (after reaching 5% stiffness loss) or the life cycles were interpolated from the almost linear diagram for dynamic stiffness over cycles. Using the new stiffness losses as stop criteria leads to Woehler curves for the 90°-0°-90°- and 30°-0°-30°-specimen which are shifted to the right. Hence these curves get closer to the exclusive 0°-specimen and reduce the factors that were retrieved in the previous chapter. The 30°-0°-30°-specimen are shifted to the right a bit more than the 90°-0°-90°-specimen due to the bigger loss of stiffness after leaving the 30°-lamina away (Young's modulus set to zero) compared to the 90°-0°-90°-specimen. This means higher cycles until this stiffness loss is reached. For the 90°-0°-90° specimen the factors are almost the same. Hence, the exclusive 0°-specimen reach 20 to 30 times higher cycles than 90°-0°-90°-specimen at the same strain level. This factor must be reduced from 20 to 8 to 12 for the 30°-0°-30°-specimen.

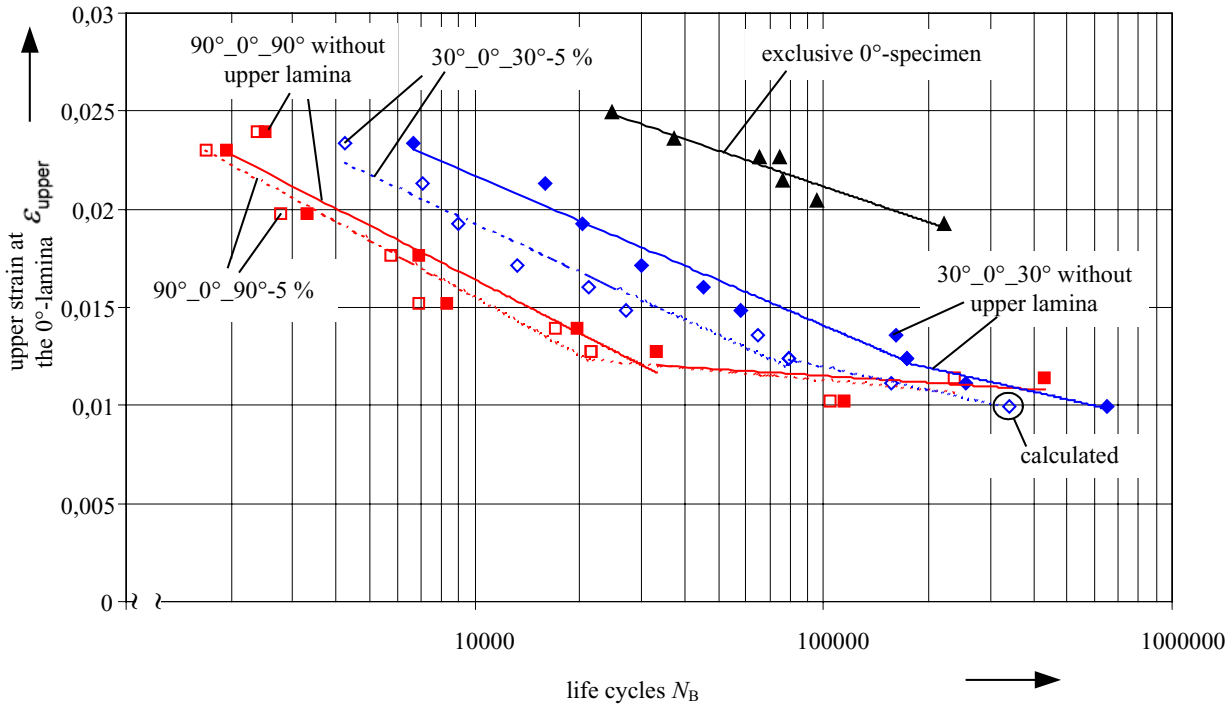

FIG 28. Woehler curves (single logarithmic) of exclusive 0°-specimen, 90°-0°-90°-specimen and 30°-0°-30°-specimen ($R = 0.1$, $f = 10\mathrm{Hz}$). Stop criterion is a loss of 5% of the specimen's dynamic stiffness (unfilled squares, dashed lines). The filled squares are values to account for the complete delamination of the upper lamina. The exclusive 0°-specimen remains untouched.

Looking at the stresses parallel to the 0°-fibres (FIG 29) a shift of the Woehler curves can be observed as well. This is valid especially for the 30°-0°-30°-specimen. For life cycle numbers of $N_B = 5 \cdot 10^3$ to $N_B = 5 \cdot 10^4$ the stress difference to the 0°-specimen accounts for $500-600\,\mathrm{N/mm^2}$ for the 90°-0°-90°-specimen and $200-350\,\mathrm{N/mm^2}$ for the 30°-0°-30°-specimen, respectively. This corresponds to a strength reduction of 35-50 % for the 90°-0°-90°-specimen and 13.5-25. % for the 30°-0°-30°-specimen, respectively. The strength of the 30°-0°-30°-specimen is not reduced as much as before (correlating to the ratio of cycles which is reduced) while the 90°-0°-90°-specimen remain at the level of strength

reduction.

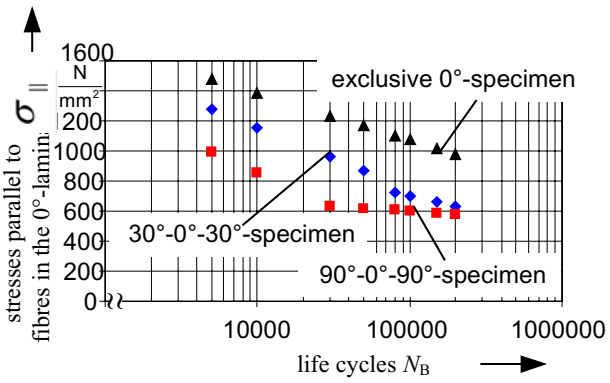

FIG 29. Stresses parallel to fibres over life cycles for worst case scenario

4. REDUCTION FACTORS FOR FATIGUE

From the FEM investigation it was observed that the length of the crack *a* and the angle between adjacent laminae are the main influencing factors on the failure of adjacent fibres. The retrieved factor between induced load and local stress increase is 1.22, i.e., the local increase of stress in the 0°-fibre accounts for 22 %.

The experimental results show a much earlier failure of a 90°-0°-90°-specimen than an exclusive 0°-specimen. The reduction of strength which is induced by IFF cracks accounts for 50 %, i.e., that a 90°-0°-90°-specimen fails at half of the stress level (under cyclic loading) which can be endured by a an exclusive 0°-specimen. Comparing FEM and experiments doesn't seem to fit initially but several reasons need to be taken into account. Firstly, FEM considers a static case and thus, the influence of the opening and closing IFF cracks during the experiments is not captured. Furthermore only one IFF crack is modelled. During the experiments the transverse lamina is saturated with IFF cracks which might lead to an even stronger effect coming from a single IFF. In a general equation the tensile fatigue strength in fibre direction, $R_{\parallel}^{+}(N)$, must be reduced. The observed reduction factor for a 90°-0°-90° laminate is

(1) $R_{\parallel 90°}^{+}(N) = 0.5 \cdot R_{\parallel}^{+}(N)$

For a 30° angle a reduced tensile fatigue strength of

(1) $R_{\parallel 30°}^{+}(N) = 0.75 \cdot R_{\parallel}^{+}(N)$

can be observed. For angles between 30° and 90° the reduction factors lie between 0.5 and 0.75. For angles lower than 30° the factor will become 1, i.e., the fatigue strength of the exclusive 0°-specimen is reached. These reduction factors match the estimated factors from *Puck* [6] and the factors from *VDI Richtlinie 2014* [5] quite well.

5. CONCLUSIONS

This work clearly shows that there is an interaction between two adjacent laminae during cyclic loading especially if one lamina is damaged by IFF cracks.

In a micro-mechanical FEM-model an IFF crack is generated at a fibre lying in a transverse angle to the load direction (0°-direction). The stress increasing influence of differential angle of a transverse and 0° lamina, the distance of the adjacent laminae and the crack length on a 0°-fibre is investigated. It is observed that the differential angle and the crack length have a major influence on the stress increase. They account for 12 % (angle) and 22 % (crack length) in the 0°-fibre.

In preliminary experimental studies the damage progress of adjacent laminae was documented with microscopy. A specimen was deflected to increasing strain levels and investigated for each resulting damage state. A characteristic damage state with a constant distance of IFF cracks and the notching effect of IFF cracks on yet undamaged 0°-fibres could be observed.

Furthermore bending fatigue tests were performed with special specimen in order to obtain Woehler curves. Uni-directional specimen (0° specimen made of prepreg), 90°-0°-90°-specimen and 30°-0°-30°-specimen (each have a thick 0°-prepreg, each thin 30°-/90° lamina made out of non-crimp fabric) were tested. The notching effect of IFF cracks on the 0°-fibres was clearly observed. Comparing 90°-0°-90°-specimen with exclusive 0°-specimen a 20 to 30 times lower life cycle is achieved. In a stress point of view the 90°-0°-90° specimen can endure $500-600\,\mathrm{N/mm^2}$ less than an exclusive 0°-specimen, i.e., this difference – induced by IFF cracks - loads the 0° lamina (in the 90°-0°-90°) additionally. This difference in stress is accounted for by reduction factors for fatigue strength. Having a differential angle of 90° and loading in 0° direction the fatigue strength for this specimen accounts for the half of the fatigue strength of an UD specimen (factor 0.5). For a differential angle of 30° the reduction factor accounts for 0.75.

6. REFERENCES

[1] J. Garbe, *Bruchhypothesen und Bruchkriterien für schwingend beanspruchte Glasfaser-Kunststoff-Verbunde*. Abschlussbericht zum DFG-Vorhaben 11 D2 Bu 325/27-1, Darmstadt, 1996

[2] Bakelite AG, Technische Information „EP Epoxidharze Bakelite® EPR 05322+EPH 778+EPC 120“

[3] Owens Corning, Technische Information „OC® SE 1500 Single-End Continuous Roving (Type 30®)“

[4] A. Knickrehm, *Zum Versagen unidirektionaler Glasfaser-Kunststoff-Verbunde bei Biegeschwell-beanspruchung*. Darmstadt, Technische Universität Darmstadt, Fb 16 Maschinenbau, Fachgebiet Konstruktiver Leichtbau und Bauweisen, Dissertation, 1999

[5] VDI-Gesellschaft Kunststofftechnik, *Entwicklung von Bauteilen aus Faser-Kunststoff-Verbund. Berechnungen*. Düsseldorf: VDI 2014 Blatt 3. - Richtlinie, 2003

[6] A. Puck, *Festigkeitsanalyse von Faser-Matrix-Laminaten: Modelle für die Praxis*. München, Wien: Hanser, 1996